INTERNATIONAL JOURNAL OF INNOVATIVE RESEARCH & DEVELOPMENT

ISSN: 2278 – 0211 (Online)

Design, Modeling And Hardware Implementation Of Mppt Controlled Grid Connected Hybrid System With Smart Tracker And Improved Power Quality

S. Sivakumar
PG Scholar, Anna University, Regional Centre-Madurai, India
P. Sathish Babu
Assistant Professor, Department of EEE, University College of Engineering, India

Abstract:

This paper proposes a unique standalone hybrid power generation system, applying advanced power control techniques, fed by four power sources: wind power, solar power, storage battery, and diesel engine generator, and which is not connected to a commercial power system. Considerable effort was put into the development of active-reactive power and dump power controls. The result of laboratory experiments revealed that amplitudes and phases of ac output voltage were well regulated in the proposed hybrid system. Different power sources can be interconnected anywhere on the same power line, leading to flexible system expansion. It is anticipated that this hybrid power generation system, into which natural energy is incorporated, will contribute to global environmental protection on isolated islands and in rural locations without any dependence on commercial power systems. This paper presents an intelligent method for maximizing power output from a solar system is desirable to increase efficiency by use of on MPPT algorithm, buck-boost operation and multifunctional smart solar tracking system. The proposed MPPT-algorithm is used to track MPPs because it performs precise control under rapidly changing atmospheric conditions.

A photovoltaic (PV) based dynamic voltage restorer (DVR) is proposed to handle deep voltage sags, swells and outages on a low voltage residential distribution system. The PV based DVR can recover sags up to 10%, swells up to 190% of its nominal value. Otherwise, it will operate as an Uninterruptable Power Supply (UPS) when the utility grid fails to supply. It is also designed to reduce the usage of utility grid, which is generated from nuclear and thermal power stations. PV based DVR system is comprised of PV system with low and high power DC–DC boost converter, PWM voltage source inverter, series injection transformer and semiconductor switches. Simulation results proved the capability of the proposed DVR in mitigating the voltage sag, swell and outage in a low voltage distribution system.

Key words: *Automatic Tracking, Buck-Boost Chopper, Grid connected Photovoltaic system, incremental conductance (Inccond), Maximum power point tracking (MPPT), Photovoltaic (PV) System, Renewable energy, solar tracker, Dump load, dump power control, low cost, stand- alone hybrid power generation system, storage battery, Dynamic voltage restorer (DVR), Voltage sag, Voltage swell, Outage, DC–DC boost converter.*

1. Introduction

Energy is the most basic and essential of all resources. All the energy we use on Earth comes from fission or fusion of atomic nuclei or from energy store in the Earth. The problem with both fission and fusion is that, they have dangerous radioactivity and side effect. Natural energy-based power generation systems are commonly equipped with storage batteries, to regulate output fluctuations resulting from natural energy variation. Therefore, it is necessary to prevent battery overcharging. As for the utility connected hybrid generation system consisting of a wind power, a solar power, and battery, the dump power is able to control to prevent overcharging the battery without dump load because of dump power transferred into the utility [1]. As for the individual power generation system, it is considered that a PV system featuring low-cost and simple control, which incorporates maximum power point tracking control that makes use of diode characteristics [2], or a PV system that features output stability with a multiple-input dc–dc converter capable of controlling the output of different power sources in combination [3], or a cascaded dc–dc converter PV system that features good efficiency along with low cost [4], or a wind turbine system that features output stability with a combination of an electric double-layer capacitor and storage battery [5], is suitable for use with hybrid power generation systems to stabilize power supply.

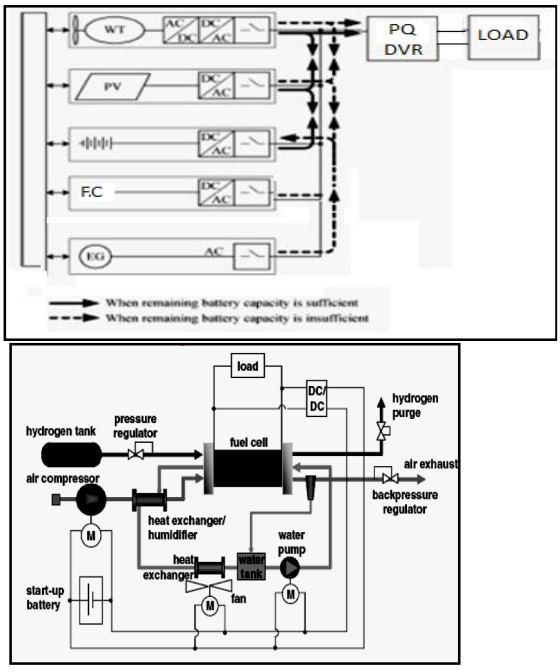

Figure 1. System operation flow

1.1 System Operation

Major operation flows of the proposed hybrid system, as shown in Fig. 1, as follows.

1) When the remaining battery capacity is sufficient: EG operation stops, and all inverters operate in parallel. Power surplus and deficit according to the balance between the output and load can be optimally adjusted through battery charging or discharging [6] – [10].

2) When the remaining battery capacity is insufficient: EG and all inverters operate in parallel. When power generated by wind and solar power generation systems is insufficient to meet load demand, EG compensates for the deficiency. Concurrently, EG charges the battery via the bidirectional inverter.

3) Fuel Cells and Energy is an electrochemical device that converts energy produced from a chemical reaction into electrical energy –This chemical reaction is not a combustion process. When the remaining fuel cell capacity is insufficient: EG and all inverters operate in parallel. When power generated by wind and solar power generation systems is insufficient to meet load demand, EG compensates for the deficiency. Concurrently, EG charges the fuel cell via the bidirectional inverter.

1.2.System Power Control Techniques

In the proposed hybrid system, we focused on how to control active-reactive power aiming at load sharing in parallel inverter operations, as well as how to control phase synchronization. Through our research activity, we devised an advanced dump power control technique without dump load [11] – [13].

1.2.1.Active-Reactive Power Control

Fig.2 shows the basic power control block diagram for the inverter section. The auto-master-slave control technique is applied in all inverters. When EG is in operation, contactor A of each inverter is closed, and these contactors are in ac-synchronized operation with all inverters that act as slaves and with EG as master. When EG operation stops, contactor B of the storage battery bidirectional inverter is closed. This inverter functions as a master and is under the constant voltage constant frequency (CVCF) condition. Contactor A of each remaining inverter acting as a slave is closed. Then, ac-synchronized operation will be underway. In studying the developmental concept of our proposed hybrid system, we focused on the mechanism of the PLL in the active-reactive power control.

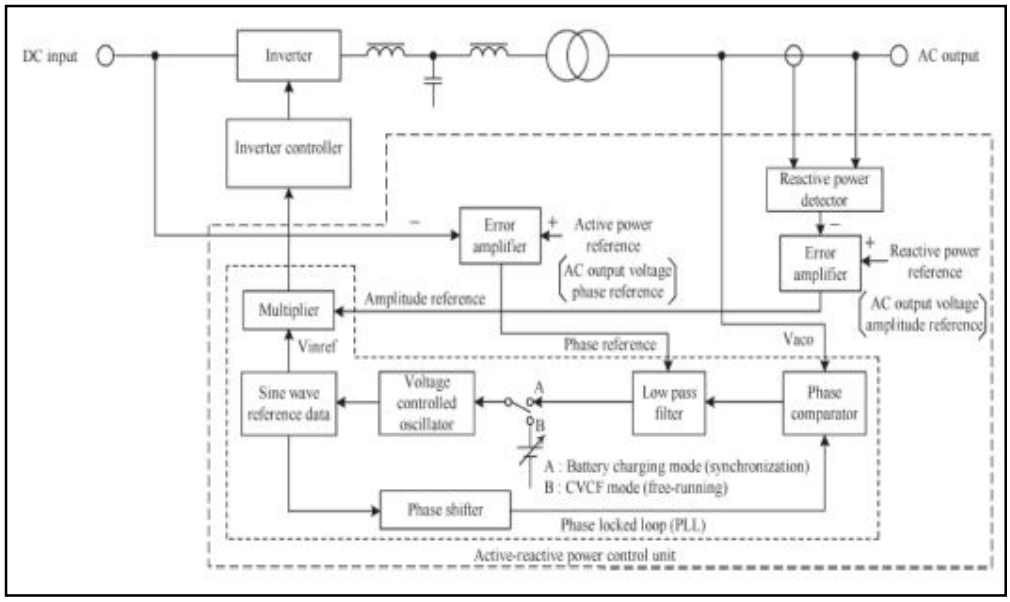

Figure 2: Basic power control block diagram of inverter section

1.2.2 Phase Locked Loop (PLL)

The PLL, which acts as a phase synchronization control, is composed of: a phase comparator, low-pass filter, phase shifter, multiplier, and voltage- controlled oscillator (VCO). The phase comparator acts to multiply the ac output voltage wave by the cosine wave reference obtained from the sine wave reference passing through the phase shifter [14]. The multiplied wave is converted to dc voltage for VCO frequency control via the low-pass filter. During synchronization with phase coincidence of the two waves (i.e., sine wave reference and ac output voltage wave), dc voltage becomes zero.

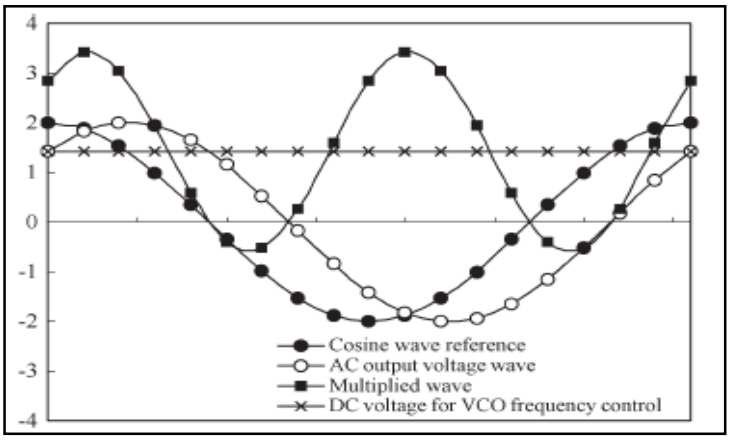

Figure 3: Synchronization with phase shift

However, during synchronization with their phase shift, dc voltage does not become zero.

Fig. 3 illustrates the individual waves and dc voltage for VCO frequency control when phase is coincident and shifted, respectively. The low- pass filter acts as an error amplifier. By giving an active power reference (i.e., ac output voltage phase reference) to the amplifier, the phase shift between sine wave reference [15] and ac output voltage wave is adjusted while synchronization is maintained in a locked state. That is, active power control is possible by altering the dc voltage.

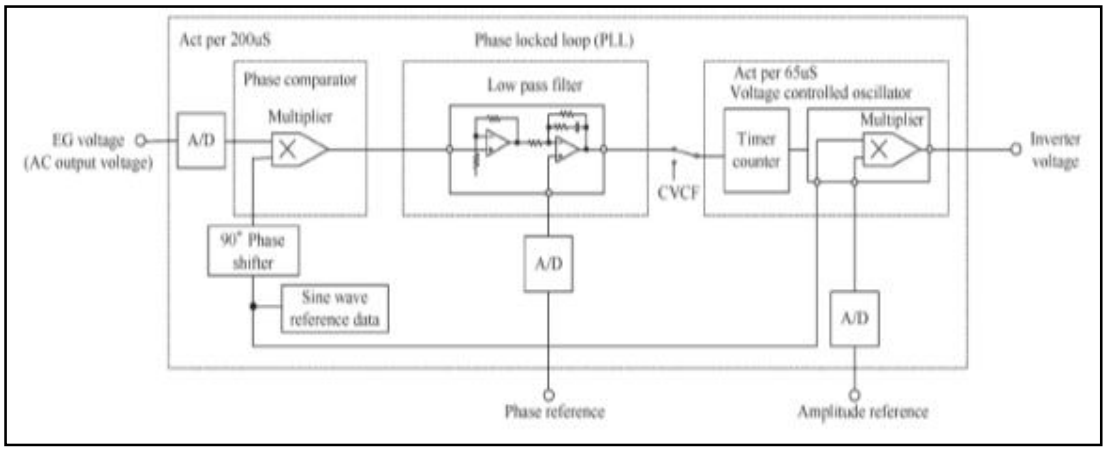

Figure 4: Detail of PLL control block diagram

Fig. 4 shows the detail of the PLL control block diagram. Two elements, that is, the phase comparator output and the phase reference signal, are imported into the low-pass filter. The output of the phase comparator is imported as synchronization data [16] (i.e., difference compared to reference frequency). The phase reference signal is imported as the amount of phase shifting in inverter output voltage while maintaining synchronization against voltage in the commercial power system. Thus, the active power varies along with the change in the phase reference signal.

For the reactive power, the sine wave reference regulated by VCO is multiplied with the signal in which the difference between reactive power reference and actual reactive power is amplified. The multiplied signal is defined as the control signal for inverter output voltage. By altering the reactive power reference, reactive power control is made possible.

1.2.3.Operation Of Parallel Inverters

We constructed a prototype standalone hybrid wind-solar power generation system, and conducted laboratory experiments. Fig. 5 shows an operating model of inverters in parallel. X1, X2, and X3 are interconnected reactors installed in WT inverter [17], PV inverter, and Bidirectional inverter, respectively. We conducted research into determination of optimal active reactive power parameters for each inverter to regulate the output under the conditions that each inverter capacity was 3 kVA (with a power factor of 0.8), and the output voltage was single phase 100 V 60 Hz. Where, active power is Psm and reactive power is Qsm at the sending-end; active power is Prm and reactive power is Qrm at the receiving-end; and the reactance of the interconnected reactor is Xm. Assuming that Vsm is defined as the sending-end voltage and Vr as the receiving-end voltage, and the angle of phase difference is δ, each of Psm, Qsm, Prm, and Qrm is represented as follows [18], [19]:

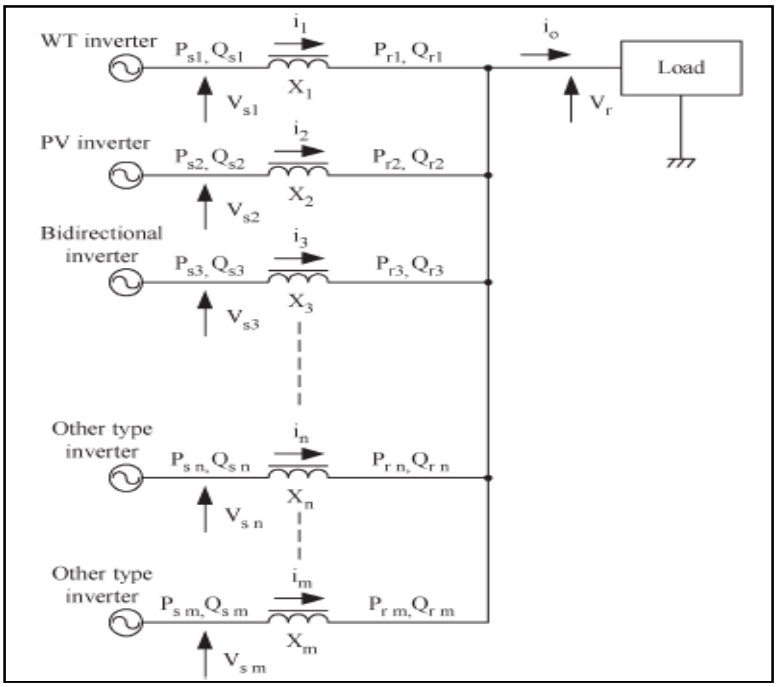

Figyre 5: Operating model of parallel inverters

$$P_{sm} = P_{rm} = \frac{V_{sm}V_r}{X_m} SIN\delta \quad (1)$$

$$Q_{sm} = \frac{V_{sm}^2 - V_{sm}V_r COS\delta}{X_m} \quad (2)$$

$$Q_{rm} = \frac{V_{sm}V_r COS\delta - V_r^2}{X_m}. \quad (3)$$

Here, m indicates the number of power sources that are operated in parallel [20]. It is desirable to regulate the voltage amplitude difference and the angle of phase difference to be within the ranges from 5 V to 15 V, and from 5° to 10° respectively.

2. Configuration And Operation Of Mppt Modules

Fig. 6 shows circuit configuration of the proposed MPPT module, of which its converter topology is a boost converter combined with a buck converter and with a shared inductor to cover a wide input voltage range upto 850 V. Input voltages V_{PV} is the output voltage of PV panels, and output voltage *VO* is the dc-bus voltage. Switch M_1 and diode D_1 act as buck-converter switches when V_{PV} is higher than V_O. On the other hand, switch M_2 and diode *D2* are acting as boost-converter switches when V_{PV} is lower than V_O. Shared inductor L_M is the main inductor and the converter is operated either in buck mode or in boost mode.

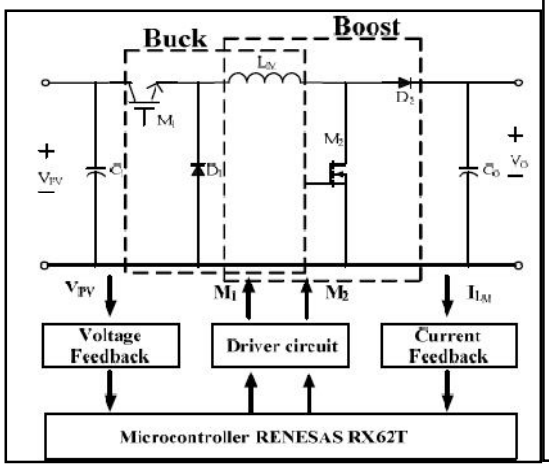

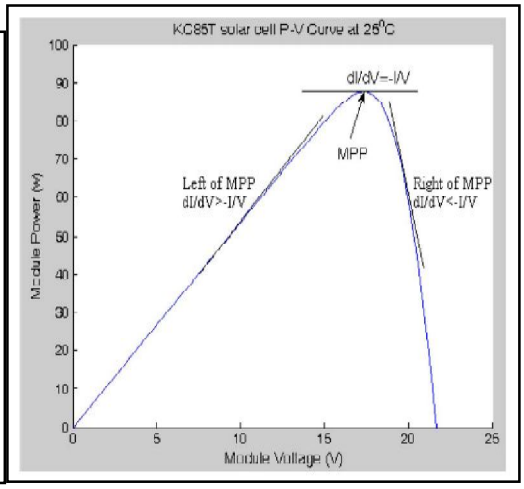

Figure 6: Proposed MPPT module *Figure 7: P-V curve of a solar module*

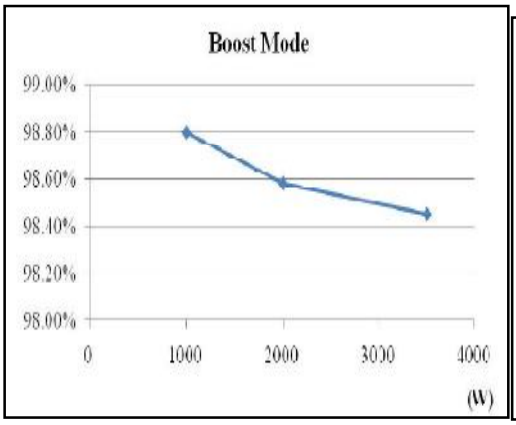

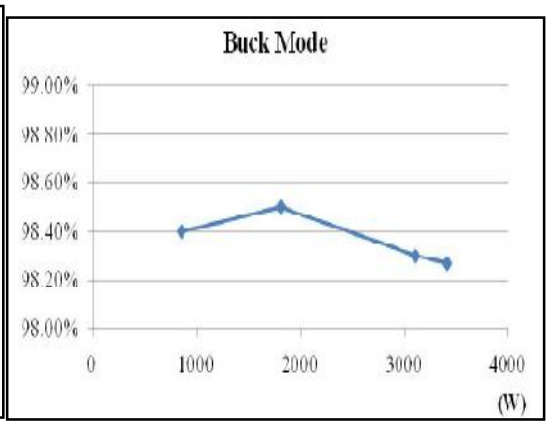

Figure 8: MPPT operated in boost mode *Figure 9: MPPT operated in buck mode*

The most critical control issue happens during the transition of buck and boost modes. When the output voltage of PV-panel string is close to the dc-bus voltage, it is hard to determine a correct operation mode and to track the maximum power points. When the pro-posed MPPT is operated in boost mode in Fig.8, since V_{PV} raises up nearly close to V_O, switch M_2 is turned off and the duty ratio of switch *M1* begins to decrease from 100%. With this control algorithm, current of PV panel i_{PV} will charge input capacitor *C1*, and *VPV* can be raised up to a higher level to prevent mode transition problems. On the contrary, switch *M1* is continuously turned on and the duty ratio of switch *M2* begins to increase from 0%, when *VPV* drops towards V_O during buck mode in Fig.9.

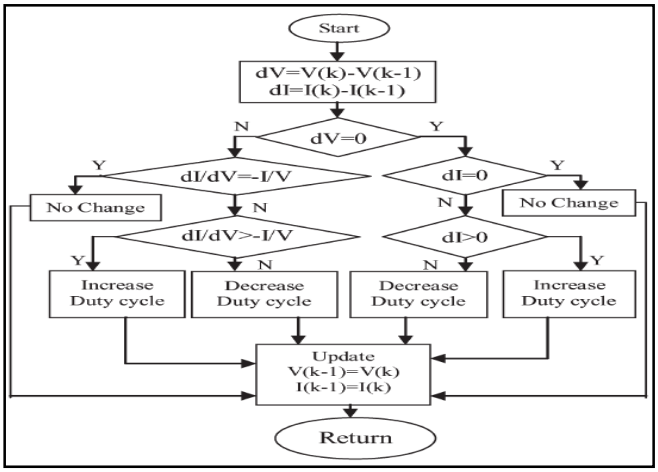

Flow chart of the proposed method with direct control

The basic equations of this method as in Fig.7 are as follows,

$$\frac{dI}{dV} = -\frac{I}{V}, \text{ at MPP} \quad (4)$$

$$\frac{dI}{dV} > -\frac{I}{V}, \text{ left of MPP} \quad (5)$$

$$\frac{dI}{dV} < -\frac{I}{V}, \text{ right of MPP} \quad (6)$$

3. Power Quality Improvement By Using Dvr

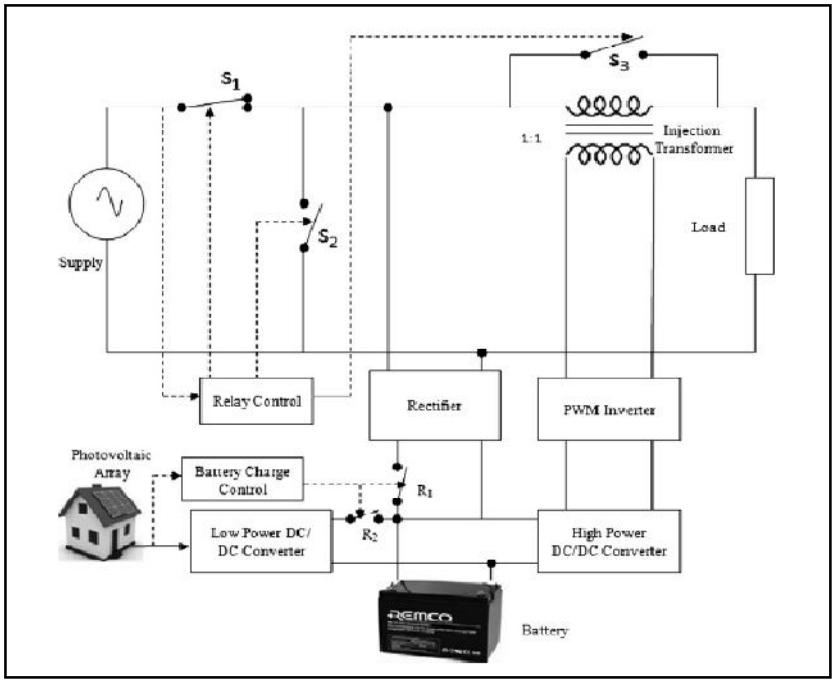

Figure 10: block diagram of the proposed PV based DVR

The block diagram of the proposed PV based DVR is shown in Fig. 10. The proposed system mainly consists of a photovoltaic array, low and high power DC/DC boost converters, battery, PWM inverter, series injection transformer, and semiconductor switches S1, S2, S3, R1 and R2.

An injecting transformer is connected in series with the load for restoring sag and swell, and is reconfigured into parallel connection using switches S1, S2 and S3 when handling outage. A DVR can compensate voltage drop across a load [22] by injecting a voltage through a series injection transformer. The injected voltage is in phase with supply voltage. In normal condition, the supply voltage is equal to the load voltage with zero angle. During sag, the supply voltage decreases to a value less than its nominal value.

The DVR reacts to the sag event and injects a compensating voltage Vinj in phase with the supply voltage to restore the voltage at nominal value. This method is very simple to implement, very fast especially in calculating the DVR compensating voltage. The injected voltage of a DVR (VDVR) can be expressed as,

$$|V_{inj}| = |V_{presag}| - |V_{sag}| \quad (7)$$

$$V_{DVR} = V_{inj} \quad (8)$$

$$\angle V_{inj} = \theta_{inj} = \theta_s \quad (9)$$

The inverter is a core component of the DVR. Its control will directly affect the dynamic performance of the DVR. A sinusoidal PWM (SPWM) scheme is used. The carrier waveform is a triangular wave with higher frequency (1080 Hz). The modulation index varies according to the input error signal from the PI controller. The basic idea of SPWM is to compare a sinusoidal control signal of normal frequency 50 Hz with a triangular carrier signal. When the control signal is greater than the carrier signal, the switches turned on and their counter switches are turned off. The output voltage of the inverter mitigates the sag, swell and outage. The DC voltage might be used from PV array if available. Otherwise, the line voltage is rectified and the DC energy is stored in batteries.

4. Standalone Solar Tracker System Modeling

4.1.Smart tracker PV Model

The smart tracker panel was installed with two LDR sensors. Assuming both sensors are placed in parallel with the PV panel, the effective irradiance is similar. As the results, the smart tracker is unable to perform the proposed sun tracking algorithm. To circumvent this, the top and bottom sensors were positioned at 45° and 135° respectively as seen in Fig 11. When the sunlight falls onto the PV panel, the LDR sensors generate different voltages (that is V_LDR_B and V_LDR_T according to the changes in the sun irradiance) to move the PV panel [21].

PV cells and the diode current is given by,

$$I = I_L - I_o\left[e^{\frac{q(V+IR_s)}{nkT}} - 1\right] \quad (10)$$

$$I_L = I_L(T_1) + K_0\left(T_{ref} - T_1\right) \quad (11)$$

$$I_L(T_1) = I_{sc}(T_1)G\left(T_{ref}\right) \quad (12)$$

$$K_0 = \frac{I_{sc}(T_2) - I_{sc}(T_1)}{T_2 - T_1} \quad (13)$$

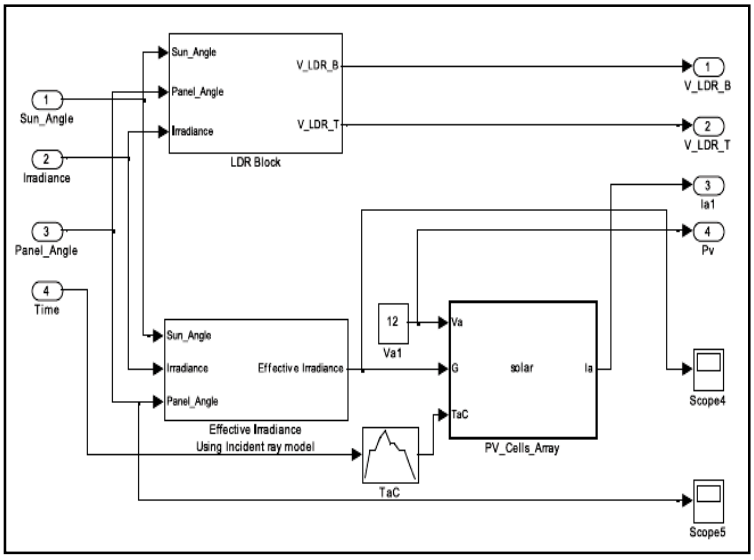

Figure 11: Smart tracker PV panel model

- Saturation current of the diode, I_0.
- Net current from the PV panel I.
- Light-generated current inside the cell IL.
- Series resistance Rs.

- Shunt resistance Rsh, in parallel with the diode.
- Diode quality factor, n;

4.2.Sun Model

At each time instant, the actual sun irradiance data obtained from the experiment was used. In the sun model, the sun is assumed to travel from 0° (sunrise) to 180° (sunset) from 7am to 5pm. During these 10 h, the PV panel rotates 180°.As shown in Fig. 12. The initial sun's angle is at 30° and with the angle changes at 15° per hour or 0.004147 per simulated time in Second; the corresponding sun angle (with respect to the base) is obtained.

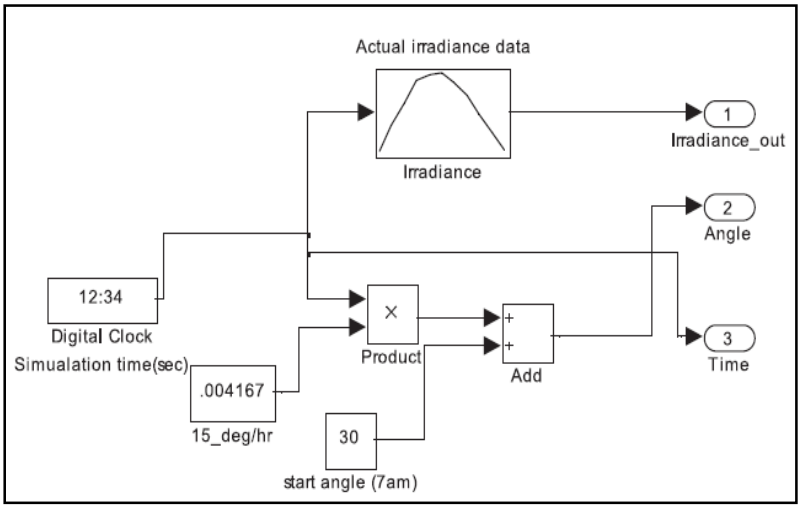

Figure 12: Sun model

5. Simulation And Experimental Results

5.1. Grid Connected Hybrid System Simulation Diagram

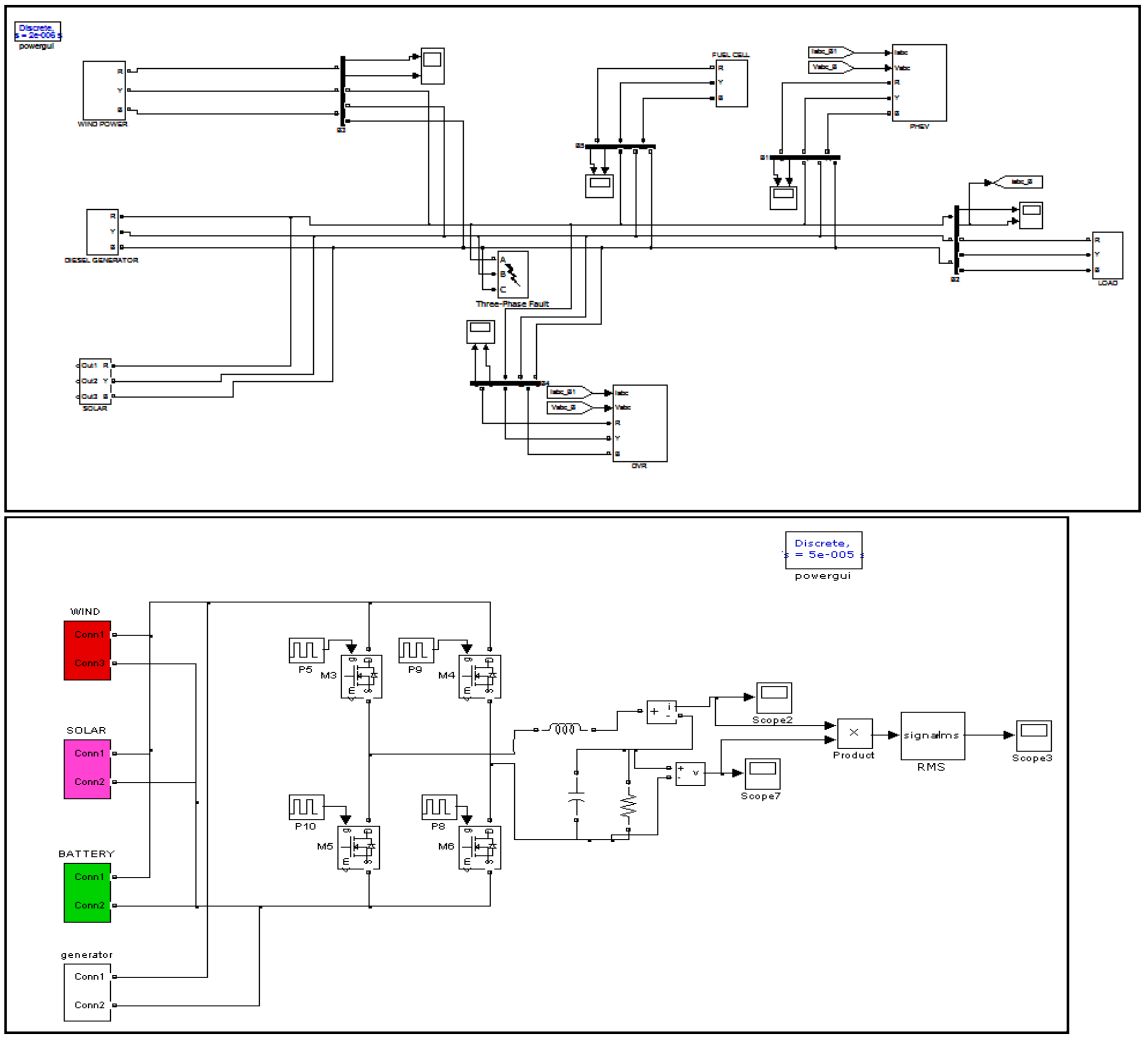

Figure 13: Grid Connected Hybrid System simulation Diagram

The proposed standalone hybrid wind-solar power generation system Fig.13 is outline composed of four power sources: a wind power generation system (with a WT converter and a WT inverter), solar power generation system (with a PV inverter), storage battery (with a bidirectional inverter), and engine generator (EG); and a control unit.

5.2.Sub System For Wind - Boost Converter

Wind output in Fig.14 AC voltage is converted into DC by full bridge rectifier circuit and C1 capacitor is used to filter the DC voltage. L12 & S2 acts as the boost converter,

D3 is freewheeling diode. Now the output voltage is rectified and boosted. In the boost converter voltage is increased but current is decreased and in the buck converter voltage is decreased but current is increased.

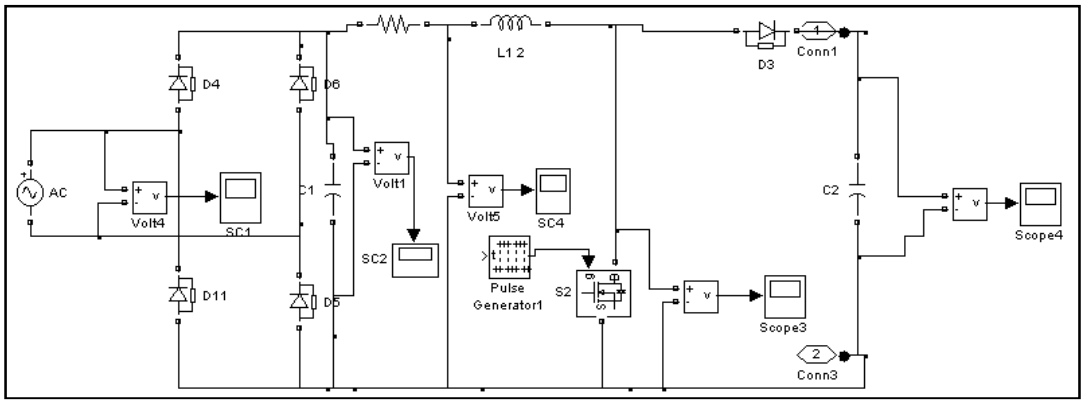

Figure 14: Wind - Boost Converter

6. Simulation Model Of Pv Based Dvr With Pi Controller

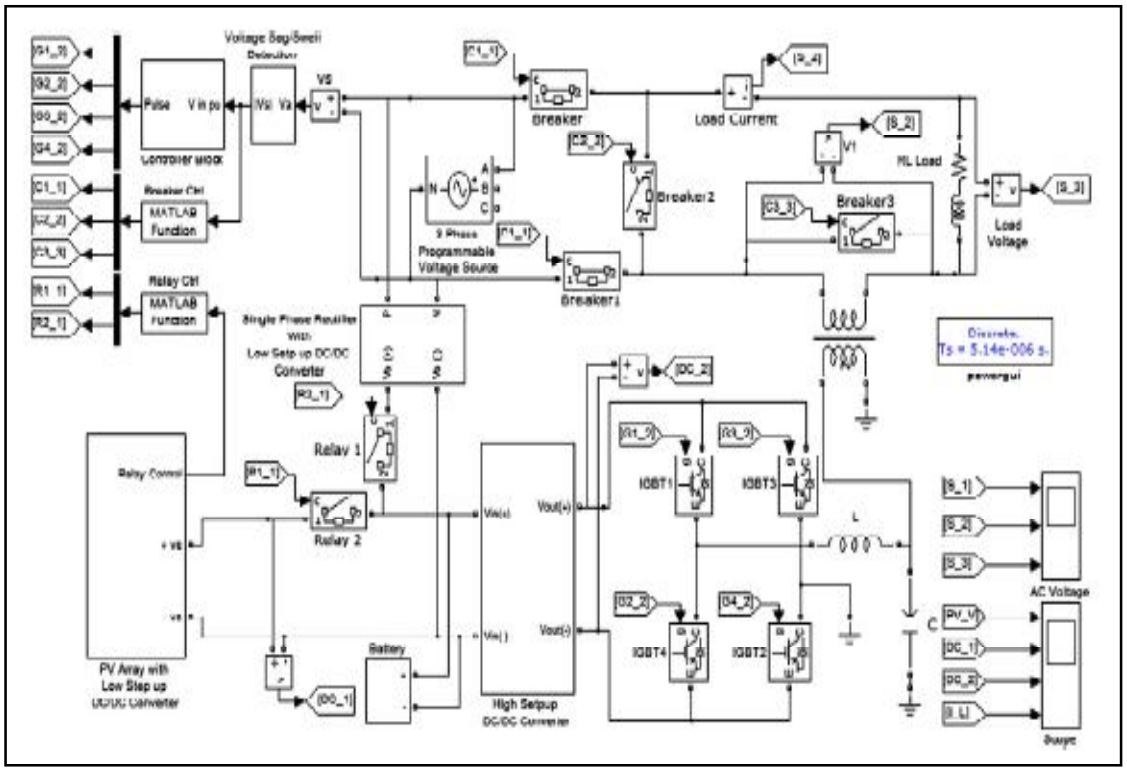

Figure 15: Simulation model of PV based DVR with PI controller

The total simulation period is 1s. Using the facilities available in MATLAB the DVR is simulated to be in operation only when the supply voltage differs from its nominal value. Otherwise, the DVR in Fig. 15 will act as online ups when the PV array output is greater

than 6 V. It reduces the energy consumption from the utility grid. When the PV array generates more power than the load demand, the excess power is stored in the battery. Therefore, during the no injection period, the generated power in the PV array charges the batteries. During the night time, the output voltage of the PV array is too low. At that time, the batteries are charged by the supply. A programmable three phase voltage source is used to provide the single phase variable voltage at the source end.

7. Stimulation Output Results

7.1.Smart Solar Tracking System

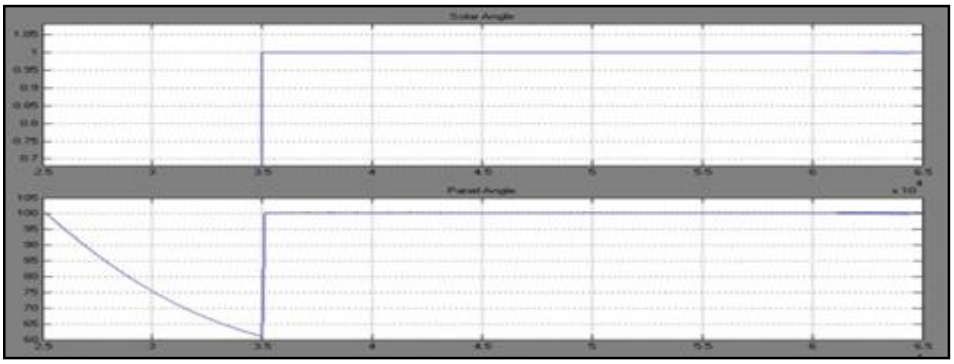

Figure 16 : Simulation results of standalone smart solar tracker

Fig. 16, shows the solar angle and panel angle with respect to time. At each time instant the actual sun irradiance data obtained from the experiment was used in the sun model, the sun assumed to travel from 0°(sun rise) to 180°(sun set).

7.2 Grid Connected Hybrid System Output

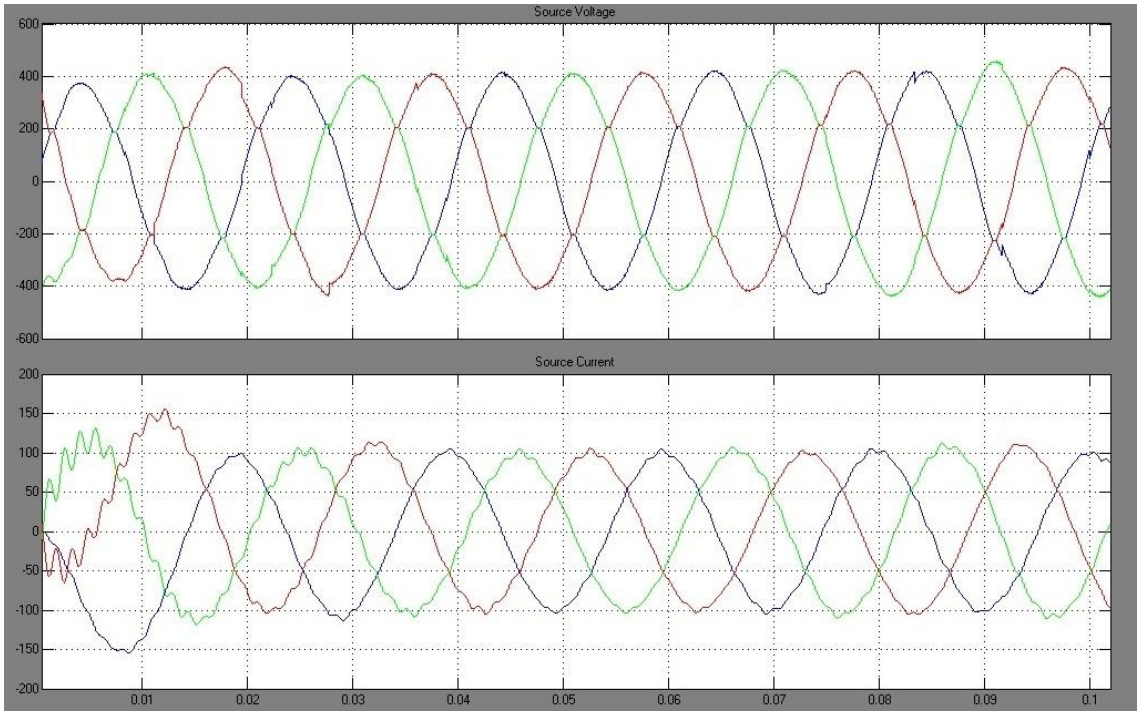

Figure 17: Source voltage and Source Current wave form

Fig. 17, shows the source voltage and source current wave form. It is combination of solar and wind. Here source voltage is 400V AC and the source current is 100A. It is a three phase input wave form.

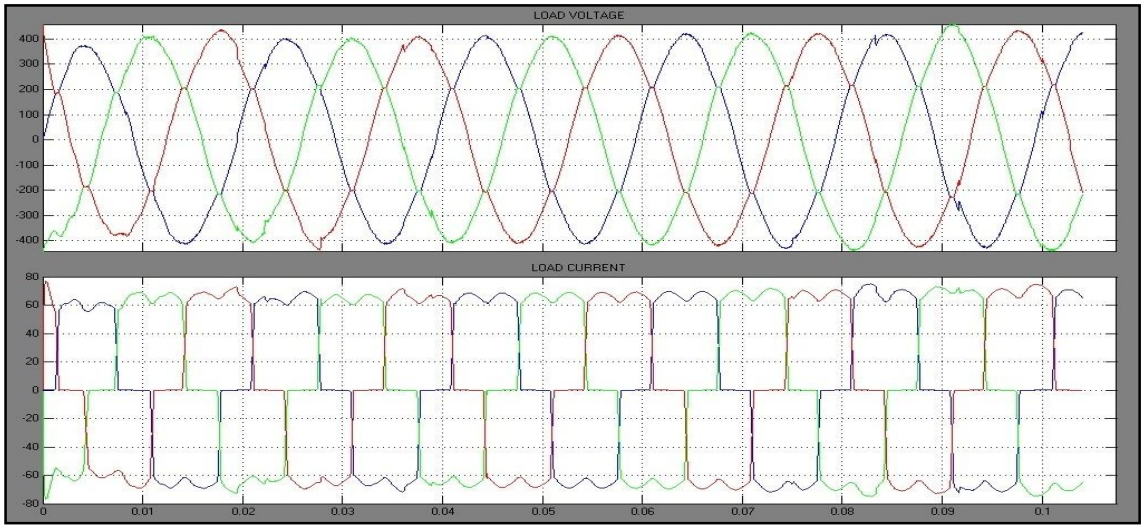

Figure 18: Load voltage and Load Current wave form

Fig. 18, shows load voltage and load current wave form. Here load is rectifier load. Load voltage is 400V AC and the load current is 70A. It is a three phase output waveform.

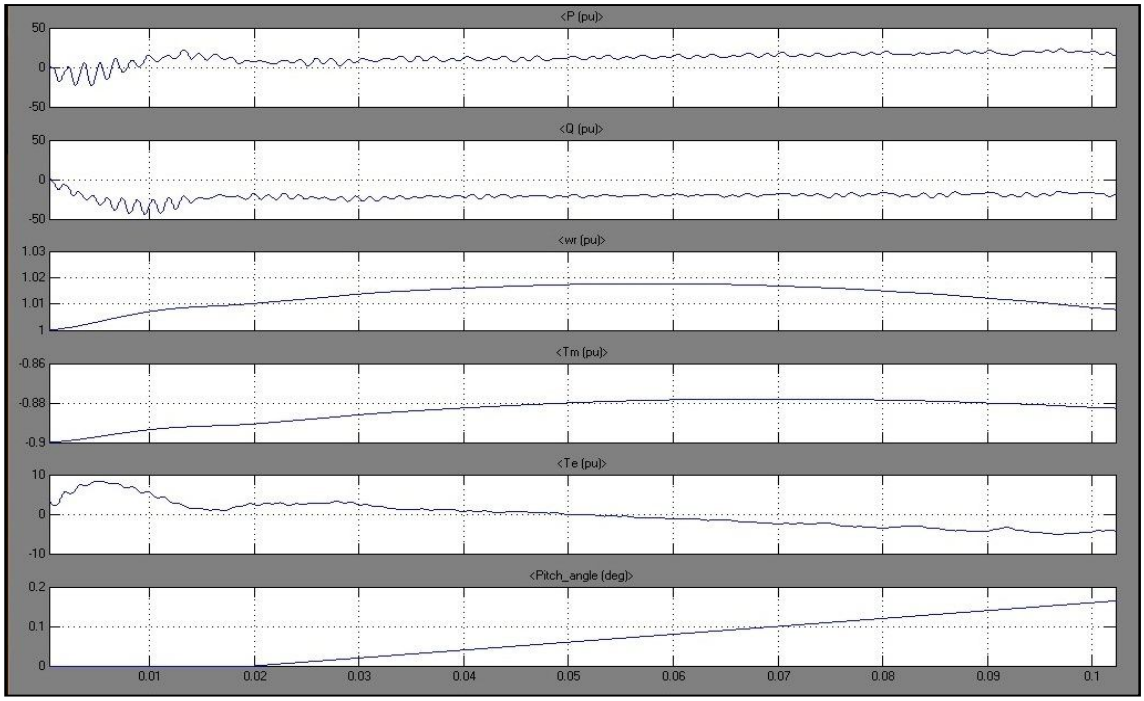

Figure 19: Data acquisition output wave form

Fig. 19, shows the data acquisition output wave form. Vabc, Iabc, wr, Tm, Te and Pitch all the parameters given to data acquisition.

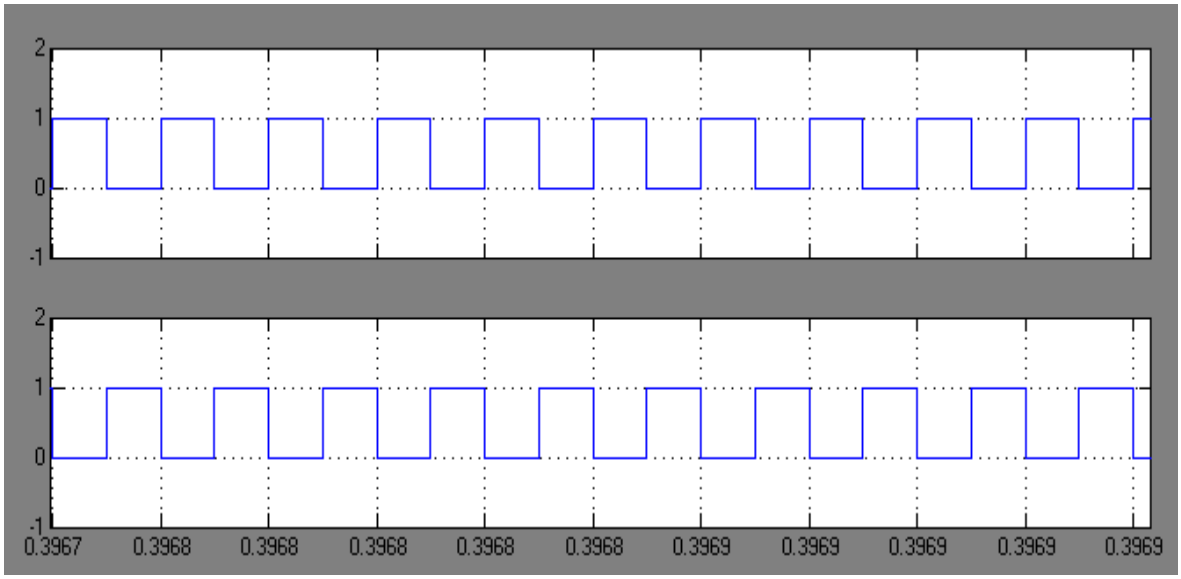

Figure 20: Inverter switching pulse for M1, M3

In Fig. 20, IGBT M3 and M6 are switched ON by the help of the triggering gate pulses P5 and P8 in the positive half cycle. In the negative half cycle M3 and M6 are switched OFF. IGBT M4 and M5 are switched ON by the help of the triggering gate pulses P9 and P10 in the positive half cycle. In the negative half cycle M4 and M5 are switched OFF.

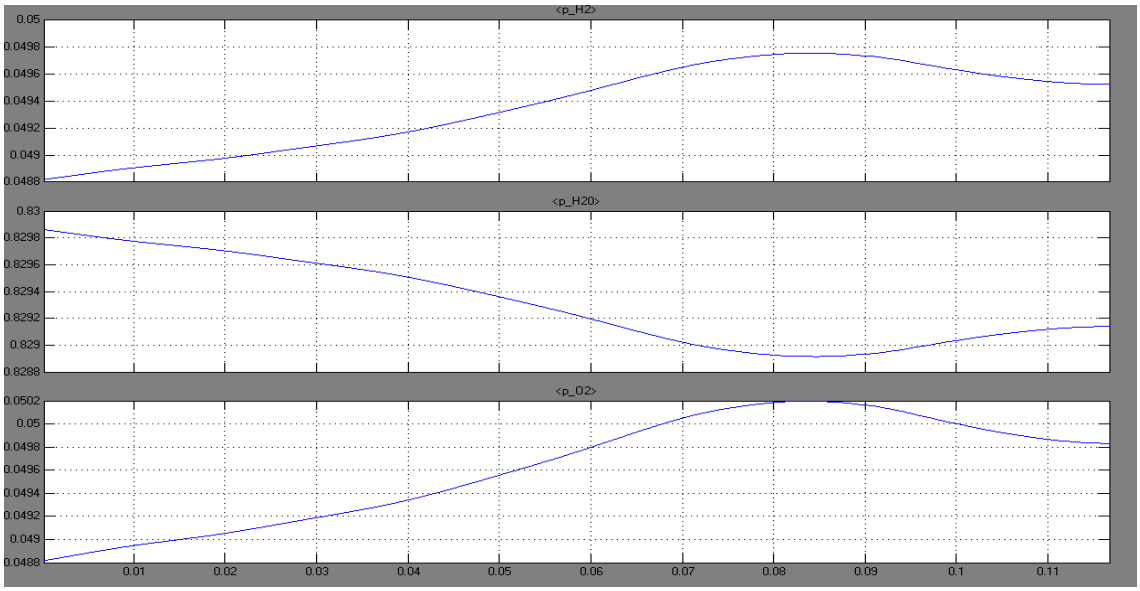

Figure 21: Fuel cell input wave form

In Fig. 21, A fuel cell is a device that uses hydrogen (or hydrogen-rich fuel) and oxygen to create electricity by an electrochemical process. If pure hydrogen is used as a fuel, fuel cells emit only heat and water as a byproduct.

7.3 DVR Supply Voltage, Injected Voltage, Load Voltage And Load Current

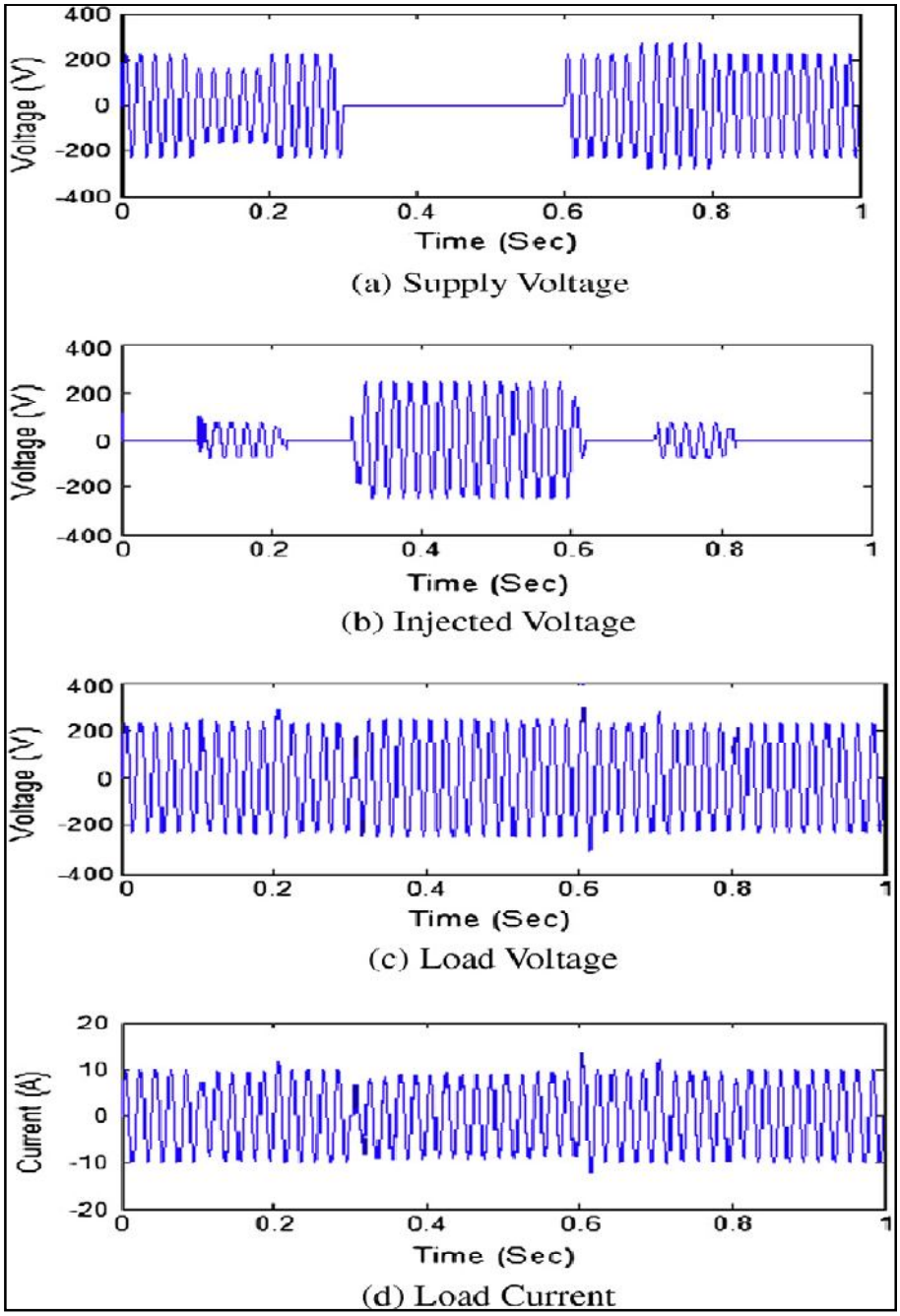

Figure 22: Supply voltage, injected voltage, load voltage and load current. (a) Supply voltage, (b) injected voltage, (c) load voltage, and (d) load current

The first simulation contains no DVR, a reduced voltage (184 V) is applied, during the period 0.1 s to 0.2 s, a raised voltage (276 V) is applied, during the period 0.7 s to 0.8 s and zero voltage (0 V) is applied, during the period 0.3 s to 0.6 s, as presented in Fig.

22a. The voltage sag and swell at the source point is 30%and 20% with respect to the reference voltage. The injected voltage, load voltage and load current of the DVR are shown in Fig. 22b–d.

8. Prototype Hybrid System

Figure 23: Prototype of the Hybrid Grid connected system with Smart Solar Tracker and DVR

9. Conclusion

This is a unique standalone hybrid wind, solar, battery and EG power generation system, which is characterized by PLL control and dump power control. In particular, dump power control allows for formation of a feedback loop in this system, meaning that there is no requirement for a dedicated high-speed line to transmit storage battery voltage and current data. In case the power line is used as a media for data transmission, the line voltage amplitudes can be applied as a means of data transmission; thus, there is no requirement for installation of any optical fiber transmission line or power line carrier system through which harmonic signals are applied to power line. In addition, neither dump load nor dump load control device are necessary. Under our dump power control, regulation of output is done without battery overcharging, and effective use of surplus power is made possible. This contributes to battery life extension and realization of a low-cost system. The system, through ac system interconnection, will also allow flexible sys- tem expansion in the future. Further, power sources including EG can be flexibly interconnected anywhere through the same power line, and power quality stability can be maintained by controlling the phase and amplitude of ac output voltage. It is expected that this hybrid system into which natural energy is incorporated, and which makes use of various power control techniques, will be applicable in rural locations, even those with poor communications media. The system will also contribute to global environmental protection through application on isolated islands without any dependence on commercial power systems.

10.Reference

1. S.-K. Kim, J.-H. Jeon, C.-H. Cho, J.-B. Ahn, and S.-H. Kwon, (2008, April), "Dynamic modeling and control of a grid-connected hybrid generation system with versatile power transfer," IEEE Trans. Ind. Electron., vol. 55, no. 4, pp. 1677–1688.
2. K. Kobayashi, H. Matsuo, and Y. Sekine, (2006, April), "An excellent operating point tracker of the solar-cell power supply system," IEEE Trans. Ind. Electron., vol. 53, no. 2, pp. 495–499.
3. K. Kobayashi, H. Matsuo, and Y. Sekine, (2006, February), "Novel solar-cell power supply system using a multiple-input dc–dc converter," IEEE Trans. Ind. Elec- tron., vol. 53, no. 1, pp. 281–286.
4. A. I. Bratcu, I. Munteau, S. Bacha, D. Picault, and B. Raison,(2011, February), "Cascaded dc–dc converter photovoltaic systems: Power optimization issues," IEEE Trans. Ind. Electron., vol. 58, no. 2, pp. 403–411.
5. [5] W. Li, G. Joos, and J. Belanger, (2010, April), "Real-time simulation of a wind turbine generator coupled with a battery supercapacitor energy storage system," IEEE Trans. Ind. Electron., vol. 57, no. 4, pp. 1137–1145.
6. [6] F. Valenciaga and P. F. Puleston, (2005, June), "Supervisor control for a stand-alone hybrid generation system using wind and photovoltaic energy," IEEE Trans. Energy Convers., vol. 20, no. 2, pp. 398–405.
7. S. Meenakshi, K. Rajambal, C. Chellamuthu, and S. Elangovan, (2006), "Intelligent controller for a stand-alone hybrid generation system," in Proc. IEEE Power India Conf., New Delhi, India.
8. R. Belfkira, O. Hajji, C. Nichita, and G. Barakat, (2007, September), "Optimal sizing of stand-alone hybrid wind/pv system with battery storage," in Proc. Power Electron. Appl. Eur. Conf., pp. 1–10.
9. S. Wang and Z. Qi, (2009, May), "Coordination control of energy management for stand-alone wind/pv hybrid systems," in Proc. IEEE ICIEA, pp. 3240–3244.
10. C. Liu, K. T. Chau, and X. Zhang, (2010, March), "An efficient wind-photovoltaic hybrid generation system using doubly excited permanent- magnet brush- less machine," IEEE Trans. Ind. Electron., vol. 57, no. 3, pp. 831–839.

11. F. Bonanno, A. Consoli, S. Lombardo, and A. Raciti, (1998, November), "A logistical model for performance evaluations of hybrid generation systems," IEEE Trans. Ind. Appl., vol. 34, no. 6, pp. 1397–1403.
12. M. H. Nehrir, B. J. LaMeres, G. Venkataramanan, V. Gerez, and L. A. Alvarado, (2000, December), "An approach to evaluate the general performance of stand-alone wind/photovoltaic generating systems," IEEE Trans. Energy Convers., vol. 15, no. 4, pp. 433–439.
13. J. M. Carrasco, L. G. Franquelo, J. T. Bialasiewicz, E. Galvan, R. C. P. Guisado, M. A. M. Prats, J. I. Leon, and N. Moreno-Alfonso, (2006, June), "Power-electronic systems for the grid integration of renewable energy sources: A survey," IEEE Trans. Ind. Electron., vol. 53, no. 4, pp. 1002–1016.
14. S. Jiao, G. Hunter, V. Ramsden, and D. Patterson, (2001, September), "Control system design for a 20 kW wind turbine generator with a boost converter and battery bank load," in Proc. PESC, pp. 2203–2206.
15. S. Tanezaki, T. Matsushima, and S. Muroyama, (2003, October), "Stand-alone hybrid power supply system composed of wind turbines and photovoltaic modules for powering radio relay stations," in Proc. IEEE INTELEC, pp. 457–462.
16. A. M. O. Haruni, A. Gargoom, M. E. Haque, and M. Negnevitsky, (2010, February), "Dynamic operation and control of a hybrid wind-diesel stand alone power systems," in Proc. IEEE APEC, pp. 162–169.
17. D. B. Nelson, M. H. Nehrir, and C. Wang, (2005, June), "Unit sizing of stand-alone hybrid wind/pv/fuel cell power generation systems," in Proc. IEEE Power Eng. General Soc. Meeting, vol. 3, pp. 2116–2122.
18. M. C. Chandorkar, D. M. Divan, and R. Adapa, (2003, January), "Control of parallel connected inverters in standalone ac supply systems," IEEE Trans. Ind. Appl., vol. 29, no. 1, pp. 136–143.
19. J. M. Guerrero, J. Matas, L. G. de Vicuna, M. Castilla, and J. Miret, (2006, October), "Wireless-control strategy for parallel operation of distributed-generation inverters," IEEE Trans. Ind. Electron., vol. 53, no. 5, pp. 1461–1470.
20. Toshiro Hirose and Hirofumi Matsuo, (2012, February), "Standalone hybrid Wind-Solar Power Generation system applying Dump power control without dump load", IEEE trans. Ind. Electron., vol. 59, no. 2, pp. 988-997.

21. C.S. Chin, A. Babu and W. McBride, (2011, April), "Design, Modeling and Testing of a standalone single axis active solar tracker using MATLAB/Simulink", Renewable Energy, Vol.36, pp. 3075 – 3090.
22. M. Ramasamy and S. Thangavel, (2011, December), "Photovoltaic based dynamic voltage restorer with power saver capability using PI controller", Electrical power and energy systems, Vol.36, pp. 51-59